Since January 2020 Elsevier has created a COVID-19 resource centre with free information in English and Mandarin on the novel coronavirus COVID-19. The COVID-19 resource centre is hosted on Elsevier Connect, the company's public news and information website.

Fish and Shellfish Immunology 80 (2018) 618–623

Contents lists available at ScienceDirect

Fish and Shellfish Immunology

journal homepage: www.elsevier.com/locate/fsi

Short communication

Preliminary investigations on the role of Drp-1 dependent mitochondrial fission in attenuating RLR downstream signaling during nervous necrosis virus infection

Rahul Krishnan*,[1], K. Jeena, Kurcheti Pani Prasad

Aquatic Environment and Health Management Division, ICAR- Central Institute of Fisheries Education, Mumbai, India

ARTICLE INFO

Keywords:
RLR pathway
Nervous necrsis virus
Mitochondrial fission
Drp-1
MAVS

ABSTRACT

Member of the dynamin family of large GTPases, dynamin-related protein 1 (Drp1) dependent mitochondrial fission is an intricate process regulating both cellular and organ dynamics. Present study shows that NNV perturbs mitochondrial dynamics by promoting Drp-1 dependent mitochondrial fission, which attenuates MAVS mediated downstream signaling. NNV infected SISS cells revealed induction in Drp1 expression and subsequent translocation into mitochondria. The level of MAVS expression was up-regulated over a period of 24 hpi and declined with the progression of NNV infection at 48 and 72 hpi confirmed by western blot and mRNA transcript analysis. Drp-1 displayed its association with fragmented mitochondria and the transcript abundance was significant post infection along with Mff. Expression levels of IRF-3 IFN-1 and Mx followed a similar pattern with abundant expression at 48 hpi and diminished expression during the further period. Importantly, silencing of Drp1 caused significant elevation in the RLR downstream molecules and reduction in viral RNA expression. These results suggest that NNV-induced mitochondrial fission serve to attenuate host RLR signaling. This provides an illustration of host–pathogen interaction in which the virus evades innate immunity by enhancing mitochondrial fission and perturbs MAVS, and the downstream molecules.

1. Introduction

Mitochondria are the most dynamic organelle in the cell that constantly undergoes fission and fusion to facilitate cellular homeostasis [1]. The fission process of the mitochondria is mediated by mitochondrial translocation of cytosolic dynamin related protein-1 (Drp-1). The recruitment of Drp1 to mitochondria is regulated by phosporylation of respective serine residues and are specifically modulated by mitochondrial outer membrane proteins like mitochondrial fission 1 (Fis1), mitochondria fission factor (Mff) [2,3]. Mitochondrial dynamics is tightly regulated in response to variations in cellular physiology such as stress, infections, and nutrient supply [4].

The innate antiviral response through the RIG-1 like receptor (RLR) pathway is oriented towards a key regulatory molecule, mitochondrial antiviral signaling protein (MAVS). Up on recognition of the viral RNA, the RLRs, Melanoma Differentiation-Associated protein 5 (MDA5) signal downstream through the MAVS by mutual caspase activation and recruitment domains [5,6]. Localized to the mitochondria, MAVS coordinates the IFN production through regulated signaling cascades [5–8]. Studies have shown that many viral proteins enhance mitochondrial fission and compromise the host immune response by preventing MAVS signaling and the majority of the mammalian viruses escape the host IFN response by targeting the MAVS [9–12]. The IFN response escape strategy used by many of the aquatic viruses are still unclear, even though, studies demonstrated that the N protein of spring viremia of carp virus (SVCV) degrades Zebra fish MAVS [13,14].

Nodaviruses are small, non-enveloped, spherical viruses with bipartite positive-sense RNA genomes that are capped but not polyadenylated comprised of two molecules of single stranded, positive polarity RNA (RNA1 and RNA2) approximately 3.1 and 1.4 kb. RNA1 encodes an approximately 100 kDa non-structural protein that has been designated RNA-dependent RNA polymerase (RdRp) or protein A. Nodavirus synthesize a sub-genomic RNA3 from the 3′ terminus of RNA1 during RNA replication which encode a B2 protein which plays a role in silencing host RNA interference [15]. Betanodavirus predominantly infect fish causing viral nervous necrosis (VNN), an infectious neuropathological disease characterized by necrosis of the central nervous system and retina [16]. VNN can induce massive death of the larval and juvenile populations of several marine teleost species including Asian seabass in India accounting for a larger mortality rate.

* Corresponding author.
E-mail address: rkcapricon@gmail.com (R. Krishnan).
[1] Present address- Department of Aqualife Medicine, Chonnam National University, Republic of Korea.

https://doi.org/10.1016/j.fsi.2018.07.003
Received 2 May 2018; Received in revised form 30 June 2018; Accepted 3 July 2018
Available online 04 July 2018

Despite their severe economic impact on the aquaculture industry, the viral molecular regulation processes and the mechanism(s) of viral pathogenesis and infection of NNV have not been well studied. Oxidative stress and presence of reactive oxygen species (ROS) induced by NNV was observed in previous studies [17,18]. Studies of Su et al. [19] reported that B2 protein of NNV increases the production of hydrogen peroxide and leads to Drp-1 activation invitro. In this study, we investigated the involvement of mitochondrial fission in the attenuation of RLR downstream signaling during NNV infection.

2. Materials and methods

2.1. Cells and virus

SISS cells derived from the Asian seabass (*Lates calcarifer*) spleen were obtained from National repository of fish cell lines (NRFC), NBFGR, India and cultured in Leibovitz L-15 media (Gibco, USA) supplemented with 10% fetal bovine serum (Gibco) 100 U/ml penicillin, and 100 g/ml streptomycin at 25 °C. Nervous necrosis virus of RGNNV genotype, isolated from infected seabass was used in the present study. Virus stocks were prepared in SISS cells and titer was determined by Reed and Muench method [20].

2.2. Mitochondrial morphology and ROS production

SISS cells cultured in Labtek chamber slides were infected with NNV using multiplicity of infection (MOI) of 0.01 in HBSS (MP Biomedicals, Ohio). Following the infection, slides were stained at 0, 12, 24, 48 and 72 hpi with 300 nM of MitoTracker® probe. The washed cells were fixed with 4% paraformaldehyde for and mounted with coverslip using Prolong Gold Antifade™ mounting reagent (Life technologies, USA). The slides were imaged using Olympus FV500 CLSM Confocal microscope. To determine the mitochondrial ROS production, confluent cells were stained with MitoSOX at a final concentration of 5 μM according to manufacturer's recommendation. Cells were allowed to load MitoSOX for 30 min and the cells were washed two times with HBSS. Cells were infected with NNV using multiplicity of infection (MOI) of 0.01 in HBSS and were imaged at 0, 6,12, 24, 48 and 72 hpi using a confocal microscope All experiment were repeated thrice.

2.3. Quantitative real-time RT-PCR

Total RNA was isolated using TRIzol (Invitrogen, USA) according to the manufacturer's instructions. cDNA was prepared from 1 to 2 mg of RNA using the Superscript II reverse transcriptase (Invitrogen) with random hexamer primers. Real time PCR reactions (50 °C for 2 min, 95 °C for 10 min, followed by 40 cycles of 95 °C for 15 s and 60 °C for 30 s and 72 °C for 10 min) were performed in triplicate using Power SYBR Green (Applied Biosystems, Foster City, CA, USA) with primers specific for NNV-RdRp, EF-1α, MAVS, IFN-1, IRF-3, MX, Drp-1, Mff and Fis-1(Table 1). Relative gene expressions were normalized to EF-1α using the formula $2^{-\Delta\Delta CT}$ ($\Delta\Delta CT = \Delta CT_{sample} - \Delta CT_{untreated\ control}$) [21].

2.4. Transfection of siRNA

siRNA was transfected into SISS cells at a concentration of 100pM with Turbofect reagent (Thermo scientific, Lithuania) according to the manufacturer's protocol. siRNA was custom synthesized at Euofins India (Table 1). The cells were incubated at 25 °C for 6 h with rocking the plate every 15 min to prevent cell drying. Immediately after siRNA treatment, the cells were infected with NNV and the cells were analyzed at different time points to monitor the expression pattern of viral transcripts and RLR downstream molecules.

Table 1
List of primers and siRNA used in the study.

Name	primer/siRNA sequence 5′-3′
Type1 interferon	F- GCCACAAGACTAACAAGAAGC
	R- GTGAGTAGAGAAGAAACCAGC
IRF-3	F-CCAATCAGGAGCGAACAGAG
	R- GGAGGGCAGAACGGAAGTTT
Mx protein	F- GACATAGCAACCACAGAGGC
	R- TCAGCCAGTTTAGGAACGGT
MAVS	F- CTCACCAGGCATCCACAAC
	R- GCGTCCAAACCCGATGCT
EF1α	F- GTTGCCTTTGTCCCCATCTC
	R- CTTCCAGCAGTGTGGTTCCA
Drp-1	F- GCAGAGTAGCGGGAAGAGTT
	R- TCCATCCACTCCGTTCTCCT
Mff	F- CCAGCTTCACGCTTTTGTGG
	R- CACTGTGTCCTTCACCGAGT
Fis-1	F- ACAGGCCCTGGAGCTAGAAA
	R- AATCCGGCCACACCTAATCC
NNV RdRp	F- GTGTCCGGAGAGGTTAAGGATG
	R- CTTGAATTGATCAACGGTGAACA
Drp-1 siRNA	GTTCGCCTTAGCTCATTCATT
Drp-1 siRNA- scrambled	GTCCCGTTTCGTCTCTAATAT

2.5. Mitochondria isolation

Following treatments (Viz, viral infected, siRNA transfected, SiRNA transfected and virus infected and mock), the cells were trypsinized and used for the isolation of mitochondria using mitochondria isolation kit (Thermo scientific, USA) according to manufacturers' instruction. Briefly, the cells were pelleted by centrifugation at 850g for 2min. To the pellet, 800 μL of Mitochondria Isolation Reagent A was added, vortexed and incubated on ice for 2min. The suspension was homogenized in a Dounce tissue grinder and 800 μL of mitochondria isolation reagent C was added and inverted several times to mix. Tubes were centrifuged at 700g for 10 min at 4 °C and the supernatant was centrifuged at 12,000g for 15 min at 4 °C. To the pellet 500 μL Mitochondria Isolation Reagent C was added and centrifuged at 12,000g for 5min. The mitochondrial pellet was maintained on ice before downstream processing.

2.6. Gel electrophoresis and immuno-blot analysis

Samples of total cell lysate or mitochondrial fraction lysate were prepared with Totex buffer (20 mM HEPES at pH 7.9, 0.35 M NaCl, 20% glycerol, 1% NP-40, 1 mM MgCl2, 0.5 mM EDTA, 0.1 mM EGTA, 50 mM NaF and 0.3 mM Na_3VO_4) containing mixture of protease inhibitors (Sigma, St. Louis, MO), Samples were incubated in protein sample buffer (final concentration: 50 mM Tris, pH 6.8, 1% SDS, 10% glycerol, 1% b-mercaptoethanol, and 0.01% bromphenol blue) for 5 min at either 95 °C before running SDS-PAGE at room temperature followed by immunoblotting with detection antibodies. Primary antibodies were identified with HRP conjugated secondary antibody (Sigma, St. Louis, MO) and DAB substrate (Amresco, USA). Primary antibodies used were polyclonal anti-MAVS, anti Phospho-DRP1 (Ser616) - p-DRP-1(Thermo scientific, USA) and anti – VDAC1.

2.7. Statistical analysis

All the experiments were carried out in triplicates and mean data with standard error of mean were incorporated for the statistical analysis. All data were analyzed by one way ANOVA with Duncan's multiple range test using SPSS 22.0 (Chicago, USA).

3. Results and discussion

To investigate the NNV- induced alterations of mitochondrial

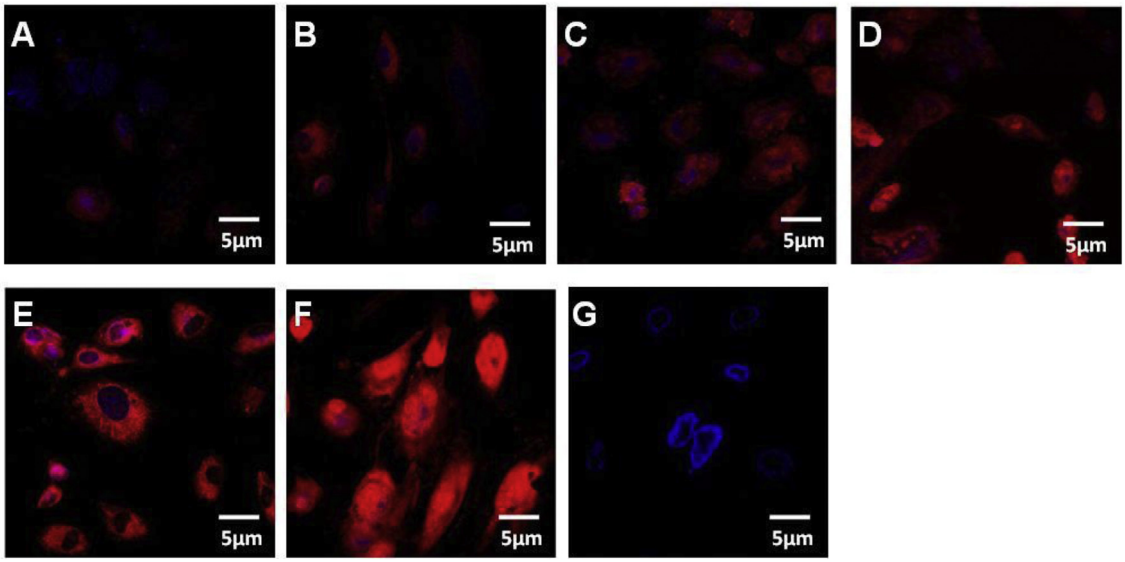

Fig. 1. NNV infection induced mitochondrial ROS production. Confocal microscopy analysis demonstrating mROS production in virus infected SISS cells stained with 5 μM of mitoSOX. A-F represents 0, 6,12,24,48 and 72 h post infection with NNV. G represents uninfected control (red-mitochondrial ROS, blue- DAPI stained nucleus).

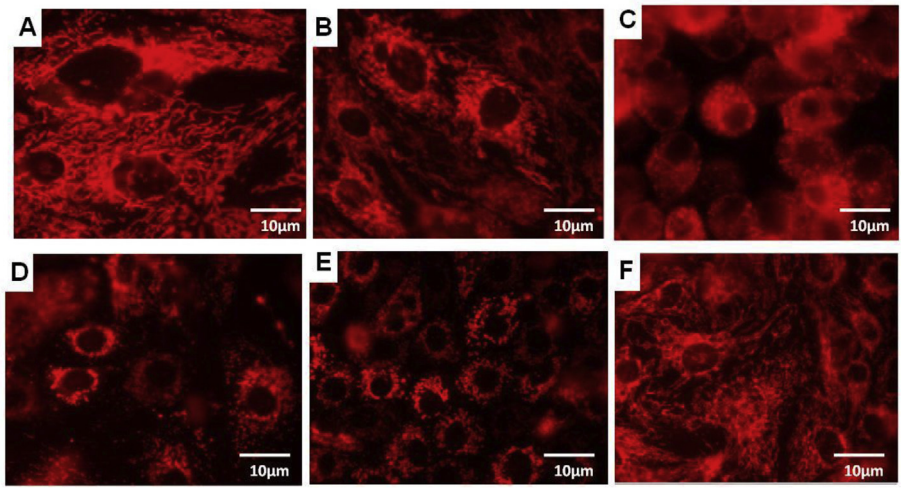

Fig. 2. NNV infection induces mitochondrial fission. Confocal microscopy analysis showing mitochondrial fission in NNV infected cells stained with 300 nm of Mitotracker red. A-E represents the extent of mitochondrial fragmentation at 0, 12,24,48,72 h post infection respectively. F represents uninfected control.

dynamics, and physiology, SISS cells were infected with cell culture-derived NNV. For studying the oxidative injury in NNV infected cells, we detected the mitochondrial superoxide production with MitoSOX™ Red, a mitochondrially localized, superoxide-sensitive fluorescent ROS indicator. As demonstrated in Fig. 1, NNV infection in the cells resulted in greater mitochondrial superoxide production compared with control in a time dependent manner. Studies have demonstrated that damaged mitochondria are potential source to initiate a vicious cycle of ROS generation and deteriorate other cellular components promoting cell death [22]. Concurrent with the present observations, HCV core protein resulted in the Ca^{2+}-dependent mitochondrial ROS production and inhibited complex I activity in Huh7 cells [23,24]. NNV infection induced oxidative stress has been reported in turbot brain, and the presence of ROS in GF-1 cells at an early stage of infection (24 h post infection, h.p.i.) induced cell death by affecting mitochondrial morphology [17,18]. As shown in Fig. 2, NNV-infected cells displayed distinct fragmented mitochondria (mitochondrial fission), in contrast to un-infected cells, which displayed a typical tubular mitochondrial network indicative of normal healthy cells. A similar result was also observed in Hepatitis B virus, Hepatitis C virus and porcine reproductive and respiratory syndrome virus [25–27].

The physiologic regulators such as mitochondrial morphology, dynamics and mitochondrial ROS also play a major role in mitochondria mediated antiviral signaling [28,29]. Mitochondrial reactive oxygen species (mROS) are being recognized as both positive and negative modulators of RLR signaling. NOX2 and ROS are reported to have a major role for triggering the host cell for efficient MAVS signaling [30]. However in the present study, as the mitochondrial ROS and fragmentation increased significantly in a time dependent manner, transcript abundance and protein expression of MAVS have shown considerable depletion in the cells (Fig. 3). Further, gene expression analysis of MAVS downstream molecules viz, IRF-3, IFN-1 and Mx have shown the significant down regulation in the mRNA transcript levels (Fig. 3C). The majority of the mammalian viruses escape the host IFN response by targeting the MAVS. In case of hepatitis C virus, enterovirus71, GBvirusB and the coxsackievirus B3, their NS3/4A serine protease, protease2Apro NS3/4A serine protease and cysteine protease 3Cpro respectively cleaves MAVS [9–12]. Studies demonstrated that the

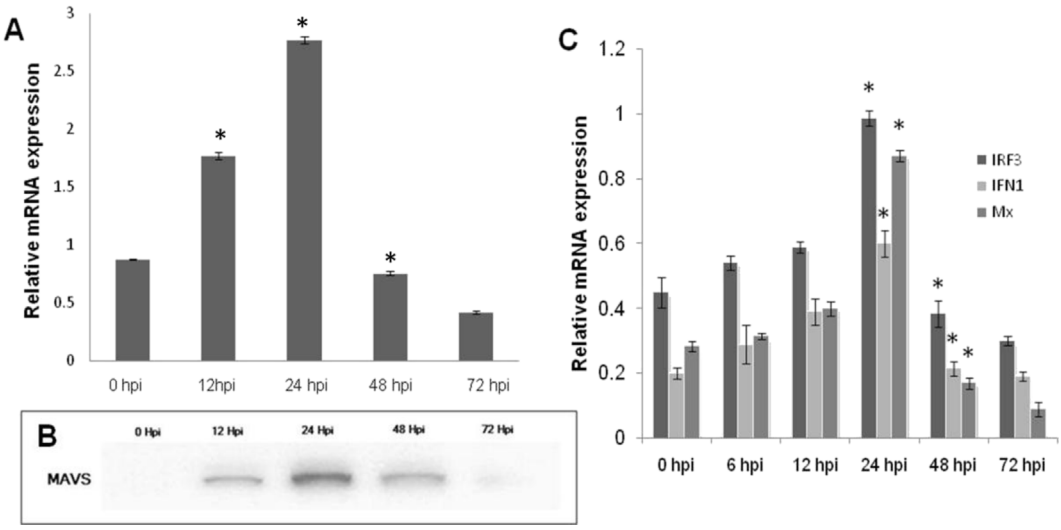

Fig. 3. Mitochondrial fission abrogates MAVS downstream signaling. A. Real time mRNA quantification of MAVS transcripts in NNV infected SISS cells at different time points. Expression was normalized with EF1α as the internal control. **B**. Western blot analysis for MAVS in mitochondrial fraction of NNV infected cells at 0-72hpi. **C**. Relative mRNA expression analysis of IRF3, IFN1 and Mx in NNV infected cells at different time point. Expression was normalized with EF1α as the internal control. Data are expressed as means with SEM of three independent experiments ($p < 0.05$), * indicates significance difference.

N protein of spring viremia of carp virus (SVCV) degrades Zebra fish MAVS by E3 ligase(s) mediated K48-linked ubiquitination [13,14]. In Contrast to these, the influenza A virus, oncolytic measles virus and the SARS corona virus dampens MAVS signaling by perturbing the mitochondrial physiology [31–33]. Thus the exact mechanism of MAVS depletion in the cells post infection with NNV needs to be addressed with more studies.

Ser616 phosphorylation of Drp-1 by cyclin B/cyclin-dependent kinase 1 (Cdk1) recruits them to mitochondria and drive the fission process [34]. To understand whether NNV induces mitochondrial fission by promoting Drp1 Ser616 phosphorylation and its subsequent translocation to mitochondria, NNV-infected cells were analyzed by using a anti-Drp1 antibody that recognizes the Ser616-phosphorylated Drp1. Confocal microscopy revealed a significant stimulation of Drp1 Ser616 phosphorylation in NNV-infected cells and most of the Ser616 phosphorylated Drp1 localized to the mitochondria (Fig. 4A). To conclude the observation that NNV induced Drp1 translocation to mitochondria, western blot analysis of mitochondrial fractions demonstrated that phosphorylated Drp1 is associated with mitochondria (Fig. 4B). Further real time expression studies stated that NNV infection increased the expression of Drp1 and Mff at mRNA level but the transcript abundance of Fis 1 remained stagnant throughout the infection (Fig. 4C). These results were in concordance with previous studies of HBV, HCV and PRSSV thus suggesting that NNV promoted Drp1 recruitment to mitochondria by stimulating Ser616 phosphorylation. To substantiate the functional role of Drp 1in mitochondrial fission, the siRNA mediated silencing of Drp 1 expression was performed. As shown in Fig. 5A, intracellular viral RNA dependent RNA polymerase (RdRp) was decreased in Drp 1deficient cells indicating the functional role of Drp1in mitochondrial fission. In similar studies on hepatitis C virus, classical swine fever virus and dengue virus, silencing of Drp1 had shown significant reduction in the viral replication as in the present study [25,35,36]. The transcript abundance of MAVS and its downstream molecules have also shown significant upregulation in Drp 1 deficient cells (Fig. 5C and D).Western blot analysis of mitochondrial fraction of NNV infected Drp 1 deficient cells shown high abundance of MAVS on mitochondria as the infection progress (Fig. 5B).

In summary our study shows that NNV stimulates the expression of Drp1 promotes its recruitment to mitochondria by stimulating the phosphorylation of Drp1 (Ser616), leading to mitochondrial fission and abrogation of MAVS downstream signaling. These preliminary observations state the functional relevance of mitochondrial dynamics in NNV infection and innate immune evasion. Further studies are required to elucidate the possible roles of other fission factors and involvement of other signaling cascades like mitophagy associated with the mitochondrial fission dynamics.

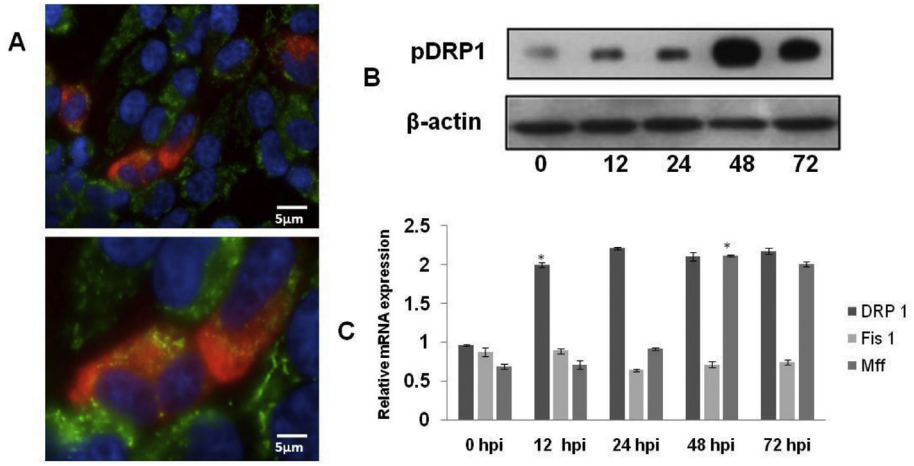

Fig. 4. NNV infection enhances Drp1 phosphorylation and its mitochondrial translocation. A. Immunofluorescence analysis at 48 hpi showing the induction of drp1 Ser616 phosphorylation in NNV-infected SISS cells. Mitochondria stained with Mitotracker green, nucleus with DAPI and anti Drp 1 probed with TRITC labeled secondary antibody. **B**. SISS cells infected with NNV and mitochondria was extracted. Association of phosporylated Drp 1 in the mitochondrial fraction determined by western blot. VDAC-1 used as mitochondrial marker. **C**. Time dependent real time mRNA expression analysis of mitochondrial fission factors in NNV infected cells. Expression was normalized with EF1α as the internal control. Data are expressed as means with SEM of three independent experiments ($p < 0.05$), * indicates significance difference.

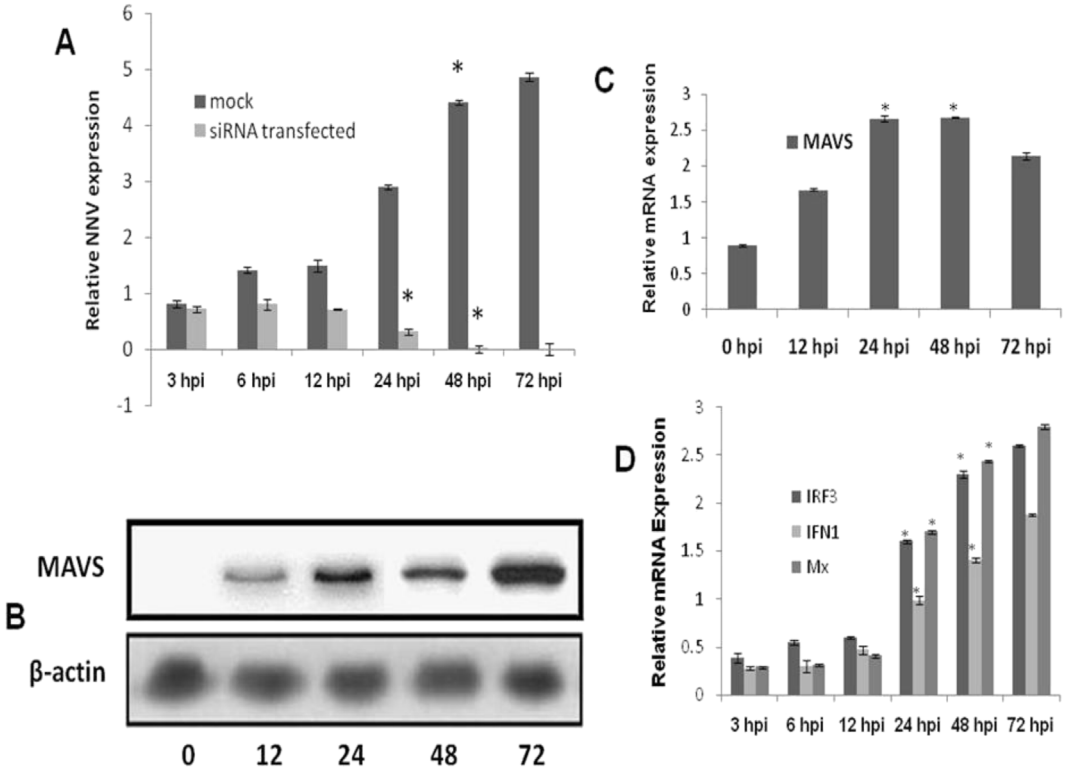

Fig. 5. Drp 1 deficiency affects NNV replication and restoration of MAVS downstream signaling. **A**. Relative mRNA expression of NNV RdRp gene in SiRNA transfected cells infected with NNV at different time points. **B**. Western blot analysis for MAVS in mitochondrial fraction of NNV infected cells (SiRNA transfected cells) at 0-72hpi.**C.** mRNA transcript abundance of MAVS in the SiRNA transfected cells at 0–72 hpi **D**. Relative mRNA expression analysis of IRF3, IFN1 and Mx in SiRNA transfected cells infected with NNV at different time points. Expression was normalized with EF1α as the internal control. Data are expressed as means with SEM of three independent experiments ($p < 0.05$), * indicates significance difference.

Acknowledgments

The authors would like to thank the director ICAR-Central Institute of Fisheries Education for providing the research platform and all the colleagues of aquatic environment and health management division of CIFE for their technical assistance. Special thanks to Dr. Vasudev for sparing the laboratory facilities used in this work.

References

[1] D.C. Chan, Fusion and fission: interlinked processes critical for mitochondrial health, Annu. Rev. Genet. 46 (2012).
[2] O.C. Losón, Z. Song, H. Chen, D.C. Chan, Fis1, Mff, MiD49, and MiD51 mediate Drp1 recruitment in mitochondrial fission, Mol. Biol. Cell 24 (2013) 659–667.
[3] H. Otera, N. Ishihara, K. Mihara, New insights into the function and regulation of mitochondrial fission, Biochim. Biophys. Acta Mol. Cell Res. 1833 (2013) 1256–1268.
[4] M. Liesa, M. Palacín, A. Zorzano, Mitochondrial dynamics in mammalian health and disease, Physiol. Rev. 89 (2009) 799–845.
[5] T. Kawai, K. Takahashi, S. Sato, C. Coban, H. Kumar, H. Kato, K.J. Ishii, O. Takeuchi, S. Akira, IPS-1, an adaptor triggering RIG-I-and Mda5-mediated type I interferon induction, Nat. Immunol. 6 (2005) 981.
[6] E. Meylan, J. Curran, K. Hofmann, D. Moradpour, M. Binder, R. Bartenschlager, J. Tschopp, Cardif is an adaptor protein in the RIG-I antiviral pathway and is targeted by hepatitis C virus, Nature 437 (2005) 1167.
[7] R.B. Seth, L. Sun, C.K. Ea, Z.J. Chen, Identification and characterization of MAVS, a mitochondrial antiviral signaling protein that activates NF-κB and IRF3, Cell 122 (2005) 669–682.
[8] L.G. Xu, Y.Y. Wang, K.J. Han, L.Y. Li, Z. Zhai, H.B. Shu, VISA is an adapter protein required for virus-triggered IFN-β signaling, Mol. Cell. 19 (2005) 727–740.
[9] X.D. Li, L. Sun, R.B. Seth, G. Pineda, Z.J. Chen, Hepatitis C virus protease NS3/4A cleaves mitochondrial antiviral signaling protein off the mitochondria to evade innate immunity, Proc. Natl. Acad. Sci. U. S. A 102 (2005) 17717–17722.
[10] Z. Chen, Y. Benureau, R. Rijnbrand, J. Yi, T. Wang, L. Warter, R.E. Lanford, S.A. Weinman, S.M. Lemon, A. Martin, K. Li, GB virus B disrupts RIG-I signaling by NS3/4A-mediated cleavage of the adaptor protein MAVS, J. Virol. 8 (2007) 964–976.
[11] A. Mukherjee, S.A. Morosky, E. Delorme-Axford, N. Dybdahl-Sissoko, M.S. Oberste, T. Wang, C.B. Coyne, The coxsackievirus B 3Cpro protease cleaves MAVS and TRIF to attenuate host type I interferon and apoptotic signaling, PLoS Pathog. 7 (2011) e1001311.
[12] A. Wang, X. Xi, X. Lei, X. Zhang, S. Cui, J. Wang, Q. Jin, Z. Zhao, Enterovirus 71 protease 2Apro targets MAVS to inhibit anti-viral type I interferon responses, PLoS Pathog. 9 (2013) e1003231.
[13] J. Yuan, Y. Yang, H. Nie, L. Li, W. Gu, L. Lin, M. Zou, X. Liu, M. Wang, Z. Gu, Transcriptome analysis of epithelioma papulosum cyprini cells after SVCV infection, BMC Genom. 15 (2014) 935.
[14] L.F. Lu, S. Li, X.B. Lu, S.E. LaPatra, N. Zhang, X.J. Zhang, D.D. Chen, P. Nie, Y.A. Zhang, Spring viremia of carp virus N protein suppresses fish IFNφ1 production by targeting the mitochondrial antiviral signaling protein, J. Immunol. 196 (2016) 3744–3753.
[15] T. Iwamoto, K. Mise, A. Takeda, Y. Okinaka, K.I. Mori, M. Arimoto, T. Okuno, T. Nakai, Characterization of Striped jack nervous necrosis virus subgenomic RNA3 and biological activities of its encoded protein B2, J. Gen. Virol. 86 (2005) 2807–2816.
[16] J.Z. Costa, K.D. Thompson, Understanding the interaction between Betanodavirus and its host for the development of prophylactic measures for viral encephalopathy and retinopathy, Fish Shellfish Immunol. 53 (2016) 35–49.
[17] A. Montes, A. Figueras, B. Novoa, Nodavirus encephalopathy in turbot (Scophthalmus maximus): inflammation, nitric oxide production and effect of anti-inflammatory compounds, Fish Shellfish Immunol. 28 (2010) 281–288.
[18] C.W. Chang, Y.C. Su, G.M. Her, C.F. Ken, J.R. Hong, Betanodavirus induces oxidative stress-mediated cell death that prevented by anti-oxidants and zfcatalase in fish cells, PLoS One 6 (2011) e25853.
[19] Y.C. Su, H.W. Chiu, J.C. Hung, J.R. Hong, Beta-nodavirus B2 protein induces hydrogen peroxide production, leading to Drp1-recruited mitochondrial fragmentation and cell death via mitochondrial targeting, Apoptosis 19 (2014) 1457–1470.
[20] L.J. Reed, H. Muench, A simple method of estimating fifty per cent endpoints, Am. J. Epidemiol. 27 (1938) 493–497.
[21] K.J. Livak, T.D. Schmittgen, Analysis of relative gene expression data using real-time quantitative PCR and the $2^{-\Delta\Delta CT}$ method, Methods 25 (2001) 402–408.
[22] L.A. Sena, N.S. Chandel, Physiological roles of mitochondrial reactive oxygen species, Mol. Cell. 48 (2012) 158–167.
[23] M. Korenaga, T. Wang, Y. Li, L.A. Showalter, T. Chan, J. Sun, S.A. Weinman, Hepatitis C virus core protein inhibits mitochondrial electron transport and increases reactive oxygen species (ROS) production, J. Biol. Chem. 280 (2005) 37481–37488.
[24] Y. Li, D.F. Boehning, T. Qian, V.L. Popov, S.A. Weinman, Hepatitis C virus core protein increases mitochondrial ROS production by stimulation of Ca2+ uniporter

activity, Faseb. J. 21 (2007) 2474–2485.
[25] S.J. Kim, M. Khan, J. Quan, A. Till, S. Subramani, A. Siddiqui, Hepatitis B virus disrupts mitochondrial dynamics: induces fission and mitophagy to attenuate apoptosis, PLoS Pathog. 9 (2013) e1003722.
[26] S.J. Kim, G.H. Syed, M. Khan, W.W. Chiu, M.A. Sohail, R.G. Gish, A. Siddiqui, Hepatitis C virus triggers mitochondrial fission and attenuates apoptosis to promote viral persistence, Proc. Natl. Acad. Sci. Unit. States Am. 111 (2014) 6413–6418.
[27] S. Li, J. Wang, A. Zhou, F.A. Khan, L. Hu, S. Zhang, Porcine reproductive and respiratory syndrome virus triggers mitochondrial fission and mitophagy to attenuate apoptosis, Oncotarget 7 (2016) 56002.
[28] J.L. Jacobs, C.B. Coyne, Mechanisms of MAVS regulation at the mitochondrial membrane, J. Mol. Biol. 425 (2013) 5009–5019.
[29] T. Koshiba, Mitochondrial-mediated antiviral immunity, Biochim. Biophys. Acta Mol. Cell Res. 1833 (2013) 225–232.
[30] A. Soucy-Faulkner, E. Mukawera, K. Fink, A. Martel, L. Jouan, Y. Nzengue, D. Lamarre, C.V. Velde, N. Grandvaux, Requirement of NOX2 and reactive oxygen species for efficient RIG-I-mediated antiviral response through regulation of MAVS expression, PLoS Pathog. 6 (2010) e1000930.
[31] T. Yoshizumi, T. Ichinohe, O. Sasaki, H. Otera, S.I. Kawabata, K. Mihara, T. Koshiba, Influenza A virus protein PB1-F2 translocates into mitochondria via Tom40 channels and impairs innate immunity, Nat. Commun. 5 (2014) 4713.
[32] M. Xia, P. Gonzalez, C. Li, G. Meng, A. Jiang, H. Wang, Q. Gao, K.M. Debatin, C. Beltinger, J. Wei, Mitophagy enhances oncolytic measles virus replication by mitigating DDX58/RIG-I-like receptor signaling, J. Virol. 88 (2014) 5152–5164.
[33] C.S. Shi, H.Y. Qi, C. Boularan, N.N. Huang, M. Abu-Asab, J.H. Shelhamer, J.H. Kehrl, SARS-coronavirus open reading frame-9b suppresses innate immunity by targeting mitochondria and the MAVS/TRAF3/TRAF6 signalosome, J. Immunol. 193 (2014) 3080–3089.
[34] A.B. Knott, G. Perkins, R. Schwarzenbacher, E. Bossy-Wetzel, Mitochondrial fragmentation in neurodegeneration, Nat. Rev. Neurosci. 9 (2008) 505.
[35] H. Gou, M. Zhao, H. Xu, J. Yuan, W. He, M. Zhu, H. Ding, L. Yi, J. Chen, CSFV induced mitochondrial fission and mitophagy to inhibit apoptosis, Oncotarget 8 (2017) 39382.
[36] L. Chatel-Chaix, M. Cortese, I. Romero-Brey, S. Bender, C.J. Neufeldt, W. Fischl, P. Scaturro, N. Schieber, Y. Schwab, B. Fischer, A. Ruggieri, Dengue virus perturbs mitochondrial morphodynamics to dampen innate immune responses, Cell Host & Microbe 20 (2016) 342–356.